Phase-transition–like behavior of strong-field classical magnetotransport in a composite medium with a periodic columnar microstructure

1999 Europhys. Lett. 45 605

(http://iopscience.iop.org/0295-5075/45/5/605)

EUROPHYSICS LETTERS 1 March 1999

Europhys. Lett., **45** (5), pp. 605-611 (1999)

Phase-transition–like behavior of strong-field classical magnetotransport in a composite medium with a periodic columnar microstructure

D. J. Bergman and Y. M. Strelniker

School of Physics and Astronomy, Raymond and Beverly Sackler Faculty of Exact Sciences Tel Aviv University, Tel Aviv 69978, Israel

(received 20 October 1998; accepted in final form 23 December 1998)

PACS. 73.50Jt – Galvanomagnetic and other magnetotransport effects (including thermomagnetic effects).
PACS. 72.80Tm – Composite materials.
PACS. 68.35Rh – Phase transitions and critical phenomena.

Abstract. – A phase-transition–like change from saturating to non-saturating behavior is found in the longitudinal bulk effective magnetoresistivity $\rho_{\parallel}^{(e)}$ along some fixed directions of a two-dimensional periodic array of long, parallel, perfectly insulating inclusions embedded in a simple, free-electron conducting host. Near the transition, $\rho_{\parallel}^{(e)}$ exhibits scaling behavior, with a scaling variable that is the ratio of two physical lengths which are tending to 0. At the transition, the local current is constrained to flow in some very narrow boundary layers.

When a periodic array of long, identical, macroscopically thick, parallel inclusions, which can be either perfect insulators or perfect conductors, are embedded in an otherwise uniform conductor, the resulting system exhibits some remarkable magnetotransport properties. In particular, when the magnetic field is applied perpendicular to the columnar axis x (*i.e.*, an "in-plane" field), and the Hall-to-Ohmic resistivity ratio of the host $H \equiv \rho_{\rm Hall}/\rho_{\rm Ohm} = \mu|\mathbf{B}| = \omega_{\rm c}\tau$ (μ is the Hall mobility, $\omega_{\rm c} = e|\mathbf{B}|/(mc)$ is the cyclotron frequency—both have the same sign as the charge e of the elementary charge carriers, τ is the conductivity relaxation time) is greater than 1, a strong, anisotropic magnetoresistance appears: Both the longitudinal and the in-plane transverse macroscopic bulk effective resistivities develop a strong dependence on the magnitude as well as on the direction of $\mathbf{B}$ [1,2]. These phenomena are remarkable in that they arise in a system where the local response is entirely describable in terms of linear, continuum, classical transport theory. This means that the local current density $\mathbf{J}(\mathbf{r})$ and electric field $\mathbf{E}(\mathbf{r}) = \nabla\phi(\mathbf{r})$ are related to each other in a point-wise fashion by means of a local conductivity tensor $\widehat{\sigma}(\mathbf{r})$, and that they are determined by solving the usual classical differential equation for the electric potential $\phi(\mathbf{r})$, namely $\nabla \cdot \widehat{\sigma} \cdot \nabla\phi = 0$, subject to appropriate boundary conditions on $\phi(\mathbf{r})$. Because of the columnar symmetry, $\widehat{\sigma}$, $\mathbf{E}$, $\mathbf{J}$ are independent of x, and furthermore E_x has the same value everywhere. In contrast with the two-dimensional character of the

heterogeneity in these systems, the transport processes are usually three-dimensional: Even if the average current density is perpendicular to x, there will usually be a local current flowing in the x-direction, which does not saturate with increasing H unless J_y has the same value everywhere in the host. This leads to a positive magnetoresistance that increases as H^2 for large H [3].

Here we study a special behavior which appears in longitudinal magnetotransport, when the volume-averaged current density $\langle \mathbf{J} \rangle$ and the magnetic field $\mathbf{B}$ lie along a low-order lattice axis, and the lateral size b of the inclusions, which are perfect insulators, is allowed to vary: It is found that a drastic change occurs at a characteristic threshold value of b, where the local current distribution changes abruptly and the strong-field magnetoresistance switches from saturating to non-saturating behavior as a function of H for $|H| \gg 1$. Near the threshold, the magnetoresistance exhibits *scaling behavior*, while at the threshold the current is restricted to flow in a *narrow boundary layer*, the thickness of which tends to 0 as $1/|H|$.

These results are obtained by exploiting a duality transformation, wherein $\mathbf{E}(\mathbf{r})$ and $\mathbf{J}(\mathbf{r})$ are rotated by 90° about the x-axis at each point. The rotated fields are used to define a dual electric field $\mathbf{E}_{\rm D}$ and dual current density $\mathbf{J}_{\rm D}$

$$\mathbf{E}_{\rm D} \equiv (E_x, -\rho_0 J_z, \rho_0 J_y), \quad \mathbf{J}_{\rm D} \equiv (J_x, -E_z/\rho_0, E_y/\rho_0),$$

which are then related by the local dual conductivity tensor $\widehat{\sigma}_{\rm D}$. The host and inclusions are characterized by the following resistivity tensors and dual conductivity tensors [3]:

$$\widehat{\rho}_{\rm host} = \rho_0 \begin{pmatrix} 1 & -H & 0 \\ H & 1 & 0 \\ 0 & 0 & 1 \end{pmatrix}, \qquad \widehat{\rho}_{\rm inc} = \begin{pmatrix} \rho_{\rm ins} & 0 & 0 \\ 0 & \rho_{\rm ins} & 0 \\ 0 & 0 & \rho_{\rm ins} \end{pmatrix},$$

$$\widehat{\sigma}_{\rm D\,host} = \frac{1}{\rho_0} \begin{pmatrix} 1 & 0 & H \\ 0 & 1 & 0 \\ H & 0 & 1+H^2 \end{pmatrix}, \quad \widehat{\sigma}_{\rm D\,inc} = \begin{pmatrix} 1/\rho_{\rm ins} & 0 & 0 \\ 0 & \rho_{\rm ins}/\rho_0^2 & 0 \\ 0 & 0 & \rho_{\rm ins}/\rho_0^2 \end{pmatrix},$$

where $\rho_{\rm ins}/\rho_0 \gg 1$ and $\rho_{\rm ins}/\rho_0 \gg H^2$ (in fact, since $\rho_{\rm ins}$ is the zero-field resistivity of the insulating inclusions, we can simply write $\rho_{\rm ins} = \infty$). Note that the local dissipation rates of the two problems, $W = \rho_0 \mathbf{J}^2$ and $W_{\rm D} = \mathbf{E}_{\rm D} \cdot \widehat{\sigma}_{\rm D} \cdot \mathbf{E}_{\rm D}$, are identical. However, the dual problem is conceptually simpler than the original problem, since the dual conductivity tensors are both symmetric. This is especially useful when $|H| \gg 1$, in which case the dual host is an extremely anisotropic conductor, with the largest principal conductivity (approximately H^2/ρ_0) along an axis that is nearly the same as z, which lies along $\mathbf{B}$, while the dual inclusions are perfect conductors in both the y- and z-directions. When the periodic array of inclusions is simple (*e.g.*, a square array of circular cylinders or square–cross-section rods), and when $\mathbf{B}$ and $\langle \mathbf{J} \rangle$ lie along a low-order lattice axis, the asymptotic current distribution can often be found in closed form, using intuitive physical considerations based on the properties of the dual problem [3,4].

A surprising conclusion from the above-mentioned studies was that under boundary conditions of longitudinal transport, *i.e.*, when $\langle \mathbf{J} \rangle \parallel \mathbf{B} \parallel z$, the strong-field behavior of the system depends on whether there exist inclusion-free parallel-slab–shaped regions along $\mathbf{B}$ in the host, which span the system from end to end. If such regions exist, then the local current flow is

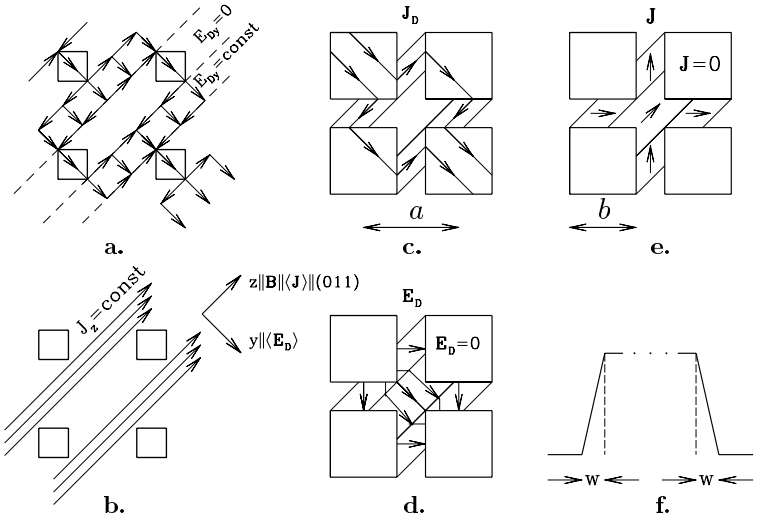

Fig. 1. – (a) and (b): Local current and field pattern (schematic) for perfectly insulating rod-shaped inclusions when (011) $\parallel \langle \mathbf{J} \rangle \parallel \mathbf{B}$ and $2b < a$. (c)–(e) Similar drawings for the case $2b > a$. (f) Trapezoidal ansatz used to describe the spatial dependence of fields and currents in the transition layers.

entirely confined to those regions, where it is uniform and parallel to z—see fig. 1(b). By contrast, when such regions do not exist, then the local current flow is extremely distorted, and has a nonzero y-component, as well as a nonsaturating component along the x-axis—see fig. 1(e). In both cases, the current distributions can be found by first considering the dual problem, which has an in-plane average electric field that is perpendicular to $\mathbf{B}$, $\langle \mathbf{E}_{\mathrm{D}} \rangle \parallel y \perp \mathbf{B}$, therefore dual current must flow in that direction—see figs. 1(a) and (c). The asymptotic in-plane dual current distribution is then found by noting that, a) wherever it can, $\mathbf{J}_{\mathrm{D}}$ always flows through the inclusions, where the in-plane dual conductivity is infinite, b) when it has to flow in the host in order to get from one inclusion to its neighbor, $\mathbf{J}_{\mathrm{D}}$ prefers to do that along z, where the dual conductivity is very large ($\sim H^2$). The in-plane components of $\mathbf{J}_{\mathrm{D}}$ are easily translated into in-plane components of $\mathbf{E}_{\mathrm{D}}$, and when those are rotated back by 90°, they yield the in-plane components of $\mathbf{J}$.

In the case of a square array ($a \times a$) of infinitely long, perfectly insulating, parallel, square–cross-section ($b \times b$) rods, when $\langle \mathbf{J} \rangle \parallel \mathbf{B} \parallel (011)$, these considerations lead to simple, closed-form expressions for the asymptotic current distributions, which are shown schematically in figs. 1(a), (b), (c), and (e). The asymptotic longitudinal magnetoresistivity, which follows from these distributions, is given by [4]

$$\frac{\rho_{\parallel}^{(\mathrm{e})}}{\rho_0} \cong \begin{cases} \dfrac{a}{a-2b}, & 2b < a, \\ \dfrac{H^2}{2}\dfrac{2b-a}{a-b}, & 2b > a. \end{cases} \tag{1}$$

Clearly, the local current distribution, as well as the macroscopic response, undergo a drastic change when $2b = a$. We now examine the detailed properties of such a threshold.

It is evident from fig. 1 that, away from the transition point, the important components of $\mathbf{J}$ are spread over a finite fraction of the unit cell, and change abruptly at the edges of those

regions. (In the case under consideration, where the inclusions have a square cross-section, those components are actually uniform wherever they are nonzero.) The transition or boundary layers at those edges have a thickness of order $a/|H|$, and they do not contribute to the macroscopic resistance in leading order [4]. However, in the close vicinity of the threshold, when the two expressions in eq. (1) have similar magnitudes, we can expect that the currents in the transition layers become important. This happens when the thickness of the inclusion-free slabs of figs. 1(a), (b), or that of the parallelogram-shaped regions in the inter-inclusion gaps of figs. 1(c), (e), becomes comparable to that of the transition layers, *i.e.*, when $|2b-a| \approx a/|H|$.

In order to study the system behavior in a way that is not totally invalidated in that regime, we now use a simple trapezoidal ansatz for the dual current profile in the transition layers, as shown in fig. 1(f). That profile, which assumes a linear change of the relevant current density component from a finite value to 0 over a fixed transition layer thickness w, describes $J_{\mathrm{D}y}(y)$ when $2b < a$, and $J_{\mathrm{D}z}(y)$ when $2b > a$.

When $2b < a$, this ansatz is expressed by

$$E_{\mathrm{D}y} = \rho_0 J_{\mathrm{D}y} \cong \begin{cases} \rho_0 \langle J_{\mathrm{D}y} \rangle, & \dfrac{b}{\sqrt{2}} < |y| < \dfrac{a}{\sqrt{8}}, \\ \rho_0 \langle J_{\mathrm{D}y} \rangle \dfrac{|\delta y|}{w}, & |\delta y| < w, \\ 0, \qquad \text{elsewhere} \end{cases} \tag{2}$$

in one unit cell ($|y| < a/\sqrt{8}$, $|z| < a/\sqrt{2}$, y and z are both measured from the inclusion center, δy is the difference between y and any one of the edges at $y = \pm b/\sqrt{2}$ or $y = \pm a/\sqrt{8}$—see fig. 1(a)). In order to find $E_{\mathrm{D}z}$ in the transition layers (it vanishes everywhere else), we use $\nabla \cdot \mathbf{J}_{\mathrm{D}} = 0$ in order to write

$$\frac{\partial J_{\mathrm{D}z}}{\partial z} = -\frac{\partial J_{\mathrm{D}y}}{\partial y} \cong \pm \frac{\langle J_{\mathrm{D}y} \rangle}{w}, \quad |\delta y| < w. \tag{3}$$

Integration of this equation leads to

$$E_{\mathrm{D}z} = \frac{\rho_0 J_{\mathrm{D}z}}{1+H^2} \cong \pm \frac{\rho_0 \langle J_{\mathrm{D}y} \rangle}{1+H^2} \frac{z}{w}, \quad |\delta y| < w. \tag{4}$$

The average of the dual dissipation rate is now calculated using eqs. (2), (4), and the fact that $E_{\mathrm{D}x} = E_x = \rho_0(\langle J_x \rangle - \langle H J_y \rangle) = 0$

$$\frac{\langle W_{\mathrm{D}} \rangle}{\rho_0 \langle J_{\mathrm{D}y} \rangle^2} \cong 1 - \frac{2b}{a} + \frac{2\sqrt{2}}{3}\frac{w}{a} + \frac{\sqrt{2}}{3}\frac{a}{wH^2}. \tag{5}$$

The variational property of $\langle W_{\mathrm{D}} \rangle$ is exploited by choosing $w = a/(\sqrt{2}|H|)$, which minimizes that quantity. In order to calculate $\rho_{\parallel}^{(\mathrm{e})}$, we note that

$$\langle J_z \rangle = -\frac{1}{\rho_0} \langle E_{\mathrm{D}y} \rangle \cong -\langle J_{\mathrm{D}y} \rangle \left(1 - \frac{2b}{a} + \frac{1}{|H|} \right), \tag{6}$$

therefore

$$\frac{\rho_{\parallel}^{(\mathrm{e})}}{\rho_0} = \frac{\langle W \rangle}{\rho_0 \langle J_z \rangle^2} \cong \frac{1 - \frac{2b}{a} + \frac{4}{3|H|}}{\left(1 - \frac{2b}{a} + \frac{1}{|H|} \right)^2}. \tag{7}$$

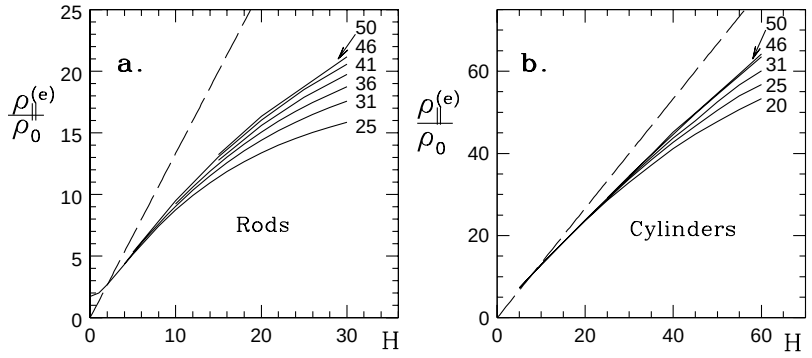

Fig. 2. – Numerical results for $\rho_{\parallel}^{(e)}/\rho_0$ *vs.* H (solid lines) of (a) a square array ($a \times a$) of rods, (b) a similar array of cylinders, at the appropriate threshold for $\mathbf{B} \parallel (011)$, using different maximal reciprocal lattice vectors—numbers show the largest integer multiple N of $2\pi/a$. Also shown, as a dashed straight line, is the approximate asymptotic prediction $4|H|/3$.

When $2b > a$, the trapezoidal ansatz leads to the following expression for $E_{\mathrm{D}z}$ in one unit cell:

$$E_{\mathrm{D}z} = \frac{\rho_0 J_{\mathrm{D}z}}{1+H^2} \cong \pm \frac{\langle E_{\mathrm{D}y}\rangle}{2(1-b/a)} \begin{cases} 1, & \dfrac{a-b}{\sqrt{2}} < |y| < \dfrac{b}{\sqrt{2}}, \\ |\delta y|/w, & |\delta y| < w. \end{cases} \tag{8}$$

The other nonzero component of $\mathbf{E}_{\mathrm{D}}$, $E_{\mathrm{D}y}$, is of order $\langle E_{Dy}\rangle$ over most of the host sub-volume. However, its most important values are much greater than that and are attained inside the transition layer, where $\nabla \times \mathbf{E}_{\mathrm{D}} = 0$ leads to

$$\frac{\partial E_{\mathrm{D}y}}{\partial z} = \frac{\partial E_{\mathrm{D}z}}{\partial y} \cong \pm \frac{\langle E_{\mathrm{D}y}\rangle}{2(1-b/a)} \frac{1}{w}. \tag{9}$$

From this we get, by integration,

$$E_{\mathrm{D}y} \cong \pm \frac{\langle E_{\mathrm{D}y}\rangle}{2(1-b/a)} \frac{z}{w}, \quad |\delta y| < w, \tag{10}$$

and consequently

$$\frac{\rho_0 \langle W_{\mathrm{D}}\rangle}{\langle E_{\mathrm{D}y}\rangle^2} \cong \frac{\sqrt{8}}{3}\left(1-\frac{b}{a}\right)\frac{a}{w} + \frac{aH^2}{a-b}\left(\frac{b}{a} - \frac{1}{2} + \frac{\sqrt{2}}{3}\frac{w}{a}\right). \tag{11}$$

Using the minimum value of $\langle W_{\mathrm{D}}\rangle$, obtained when $w = \sqrt{2}(a-b)/|H|$, plus the fact that $\langle J_z\rangle = -\langle E_{\mathrm{D}y}\rangle/\rho_0$, we now get

$$\frac{\rho_{\parallel}^{(e)}}{\rho_0} = \frac{\langle W\rangle}{\rho_0 \langle J_z\rangle^2} \cong H^2 \frac{\frac{b}{a} - \frac{1}{2}}{1-\frac{b}{a}} + \frac{4}{3}|H|. \tag{12}$$

The predictions of eqs. (7) and (12) away from the threshold, where $|1-2b/a| \gg 1/|H|$, agree with eq. (1). They are asymptotically accurate, and they compare well with numerical computations of $\rho_{\parallel}^{(e)}$ at large finite values of H [4]. By contrast, the predictions of eqs. (7)

and (12) when $|1 - 2b/a| \leq 1/|H|$ are approximate, because they depend on the precise profile assumed for the local fields in the transition layers. Comparison with numerical computations is also more difficult: Those are based on a Fourier series expansion of the local fields [1,5]. However, because the widths of the transition layers tend to 0 as $a/|H|$, the accurate representation of the fields in those layers requires higher and higher Fourier components as H increases. In fig. 2 we show results of numerical computations of $\rho_{\parallel}^{(\mathrm{e})}$ *vs.* H precisely at the threshold for several values of the largest reciprocal lattice vector $(2\pi/a)(N, N)$ that was used. Results are shown for square-rod-shaped inclusions, as well as for circular-cylinder inclusions of radius R (note that, precisely at the threshold, the trapezoidal ansatz leads to results that are independent of the inclusion shapes). It seems as though $\rho_{\parallel}^{(\mathrm{e})}$ is indeed approaching a linear dependence on $|H|$, but that the coefficient is somewhat smaller than we got using the simple trapezoidal ansatz for the field profile, and also that the coefficient is smaller for the square rods than for the cylinders. Clearly, a more accurate shape for the field profile in the transition layer is needed, one that will have to depend on the inclusion shapes.

Near the threshold, the system is characterized by two competing physical lengths, w (or $a/|H|$) and $|a - 2b|$, both of which are much smaller than the lengths a, b, $a - b$, which characterize the heterogeneous microstructure. Our calculations show that $\rho_{\parallel}^{(\mathrm{e})}$ exhibits a scaling behavior in this regime, namely

$$\frac{\rho_{\parallel}^{(\mathrm{e})}}{\rho_0} \cong \frac{a}{a-2b} F(Z), \qquad Z \equiv \frac{a-2b}{a/|H|}, \tag{13}$$

$$F(Z) = \left\{ \begin{array}{ll} \dfrac{Z^2 + 4Z/3}{(Z+1)^2}, & Z > 0, \\ -Z^2 + 4Z/3, & Z < 0, \end{array} \right\} \cong \left\{ \begin{array}{lll} 1, & |Z| \gg 1, & Z > 0, \\ -Z^2, & |Z| \gg 1, & Z < 0, \\ 4Z/3, & |Z| \ll 1, & Z \gtrless 0. \end{array} \right. \tag{14}$$

The scaling variable Z is obviously the ratio of the above-mentioned physical lengths, both of which tend to 0 at the threshold. We note that the form of $F(Z)$ for small Z is only approximate—it depends on the precise profile assumed for the fields in the transition layers. Different ansätze would lead to different values for the coefficient of Z in the last part of eq. (14), but $F(Z)$ would still be proportional to Z for $|Z| \ll 1$.

If we use the same kind of trapezoidal ansatz for the square array of circular cylinders, eq. (13) is replaced by

$$\frac{\rho_{\parallel}^{(\mathrm{e})}}{\rho_0} \cong \frac{a}{a-\sqrt{8}R} F(Z), \qquad Z \equiv \frac{a-\sqrt{8}R}{a/|H|}, \tag{15}$$

while eq. (14) remains unchanged. The transition layer thickness w has the same values as in the case of the square rods array, while $|a - \sqrt{8}R|$ is the other physical length which tends to 0 at the threshold.

Obviously, a similar discussion could be given for other micro-structural thresholds, where the thickness of the inclusion-free slabs parallel to $\mathbf{B}$ goes to 0, *e.g.*, when $\langle \mathbf{J} \rangle \parallel \mathbf{B} \parallel (01n)$ and $(1+n)b = a$, where n is any positive integer. A similar kind of threshold also exists when we consider a periodic array of perfectly conducting, parallel columnar inclusions, embedded in a normal conducting host, when $\mathbf{B}$ is perpendicular to the columnar axis and the system is subject to in-plane, transverse magnetotransport boundary conditions, *e.g.*, $\langle \mathbf{J} \rangle \parallel (01n)$ and

$\mathbf{B} \parallel (0n\overline{1}) \perp \langle \mathbf{J} \rangle$ [4, 6]. We therefore expect that similar considerations can be made and that a similar kind of behavior will appear near the threshold.

The above results are strictly valid only when the length ℓ of the columnar inclusions is infinite, $\ell = \infty$. More precisely, the requirement is $|H|\ell \gg a$ [7]. In fact, numerical calculations, as well as real experiments, have shown that, as soon as $|H|\ell \geq a$, such finite-thickness composite films already exhibit the same kind of behavior that is expected for infinite-thickness films, but with a somewhat reduced magnitude [7, 2].

It would be interesting to try and study the scaling behavior described above, both in experiments and by further numerical computations. Precisely at the threshold, a large current is constrained to flow in very narrow channels of width $w \sim a/|H|$. This may have interesting consequences that deserve further study. The possibility of inducing a large change in resistance and in local current distribution by a small change of the inclusion sizes near a threshold value may have some potential applications, particularly in view of the fact that such behavior is not based upon quantum or ballistic effects, and therefore it should be achievable at a relatively high temperature.

***

This research was supported in part by grants from the US-Israel Binational Science Foundation, the Israel Science Foundation, the Tel Aviv University Research Authority, and the Gileadi Fellowship program of the Ministry of Absorption of the State of Israel.

REFERENCES

[1] Bergman D. J. and Strelniker Y. M., *Phys. Rev. B*, **49** (1994) 16256.
[2] Tornow M., Weiss D., v. Klitzing K., Eberl K., Bergman D. J. and Strelniker Y. M., *Phys. Rev. Lett.*, **77** (1996) 147.
[3] Bergman D. J. and Strelniker Y. M., *Phys. Rev. Lett.*, **80** (1998) 3356.
[4] Bergman D. J. and Strelniker Y. M., *Phys. Rev. B*, **59** (1999) 2180.
[5] Bergman D. J. and Strelniker Y. M., *Phys. Rev. B*, **50** (1994) 14001.
[6] Fisher K. D. and Stroud D., *Phys. Rev. B*, **56** (1998) 14366.
[7] Bergman D. J. and Strelniker Y. M., *Phys. Rev. B*, **51** (1995) 13845.